

Electrochemical Study of Iridium Oxide Coating on Stainless Steel Substrate

Saeid Kakooei*, Mokhtar Che Ismail, Bambang Ari Wahjoedi

Centre for Corrosion Research, Department of Mechanical Engineering, Universiti Teknologi PETRONAS, Tronoh31750, Malaysia

*E-mail: skakooei59@hotmail.com

Received: 25 January 2013 / Accepted: 19 February 2013 / Published: 1 March 2013

Electrodeposition of Iridium Oxide (IrO₂) on stainless steel substrate was performed by cyclic voltammetry to assess its performance as pH electrode sensor. The effect of scan rate and number of cycles on IrO₂ thickness and pH sensitivity were investigated by electrochemical experiment. All fabricated pH sensor had a super-Nernstian response value in range of -69.9 to -74.5 mV/pH unit. Electrochemical results indicated iridium oxide decreased electrode impedance which was in direct relation with its thickness.

Keywords: IrO₂; pH sensor; electrodeposition; stainless steel; EIS; Cyclic voltammetry

1. INTRODUCTION

Since the past decades IrO₂ has become a preferred material for reference electrode [1, 2] and pH measurements in different fields such as biological media [3, 4], food industry [5], nuclear field [6, 7], and oil and gas industry [8-10]. Iridium oxide can provide a rapid and stable response in different media because of its high conductivity and low temperature coefficient.

Potentiometric response of the Iridium oxide to pH is a function of transition effect between two oxidation states iridium(III) oxide and iridium(IV) oxide, which can be shown as follow [11]:



The performance of iridium oxide-based electrodes, such as pH measurement, is highly dependent on deposition techniques. For example, anhydrous iridium oxides achieved by Thermal Oxidation or Sputtering Methods showed pH response of 59 mV/pH unit. However, iridium oxides fabricated by electrochemical technique are predominantly hydrated iridium oxides such as IrO₂•4H₂O,

produced a super-Nernstian response of 90 mV/pH unit [12]. Two properties of biocompatibility and corrosion resistance of iridium oxide electrodes are noticeable [13]. A crystal structure of stoichiometric iridium oxide is shown in figure 1.

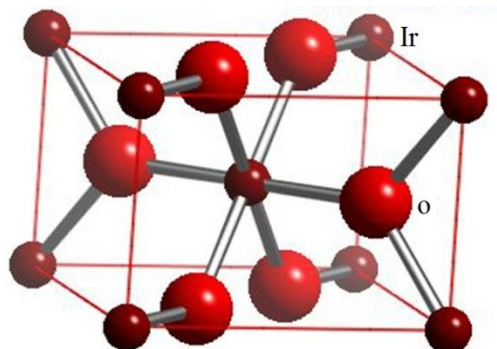


Figure 1. Crystal structure of IrO₂ [14]

Yamanaka [15] proposed electrodeposition of iridium oxide for the first time for fabrication of display device by using solution based on a complex of IrCl₄ and oxalate component. Subsequently many researchers followed and improved the solution as described by Yamanaka [16-19]. However, Marzouk [20] cautioned that using (NH₄)₂[IrCl₆] instead of IrCl₄ was wrong since the solution did not develop to dark greenish-blue colour for up to 7 days at room temperature.

Various metals have been used as substrate for electrodeposited iridium oxide film (EIROF) such as Au, Pt, Ir, PtIr, stainless steel, tin-doped indium oxide (ITO) [15, 21, 22]. Marzouk [20] in a valuable work investigated various substrate pure metals such as Au, Ag, Ti, Cu, Ni, W, Zr, and Co and some alloys such as nickel-chrome, Hastelloy and stainless steel. The blue layer of deposit, proper adhesion of deposit to surface, and stability of the cyclic voltammogram were the most important factor for substrates comparison.

Less attention was paid to stainless steel substrate which is a common and cheaper material due to possible adhesion problem. Therefore, the aim of this study is development of electrodeposition method for IrO₂ coating on stainless steel substrate.

2. EXPERIMENTAL

2.1. Chemicals and materials

Iridium(IV) chloride hydrate (IrCl₄.xH₂O) (Catalogue no. 516996); 30% hydrogen peroxide (Catalogue no. 216763); oxalic acid (Catalogue no. 75699); potassium carbonate K₂CO₃ (Catalogue no. P5833); stainless steel rods, 2.4 mm diameter; and standard pH solution buffer (4, 7, and 9) were used in this study. All chemicals were analytical reagent grade and purchased from sigma-Aldrich, USA. Distilled water was used for preparing all solution.

2.2. Preparation of IrO₂ electrode

A stainless steel rod 2.4 mm in diameter and 20 mm long was used as substrate (working electrode). Electrode was connected to a copper wire, and then mounted in Acrylic to insulate all area except a circular exposed area of 4.5 mm² for electrodeposition. The electrodes are polished by using sandpaper of different grit sizes, diamond paste and alumina powder to achieve a surface roughness of 0.5 μm. The electrodes were then rinsed and ultrasonically cleaned in acetone and deionized water.

The solution was prepared by adding 150 mg of IrCl₄.xH₂O in 100 mL of distilled water into a 200-mL glass beaker, and then followed by stirring for 10 minutes to dissolve completely. Then 360 mg oxalic acid was added to the solution and then stirred for another 10 minutes. A 1-mL of 30% hydrogen peroxide was added, and then solution was left for 15 min stirring. The pH of the solution was increased slowly to pH 10.5 by adding anhydrous potassium carbonate [15]. A light green solution was obtained. The solution was allowed to age for two days in an air-conditioned laboratory to achieve a dark blue stable solution. The schematic of the preparation is shown in figure 2.

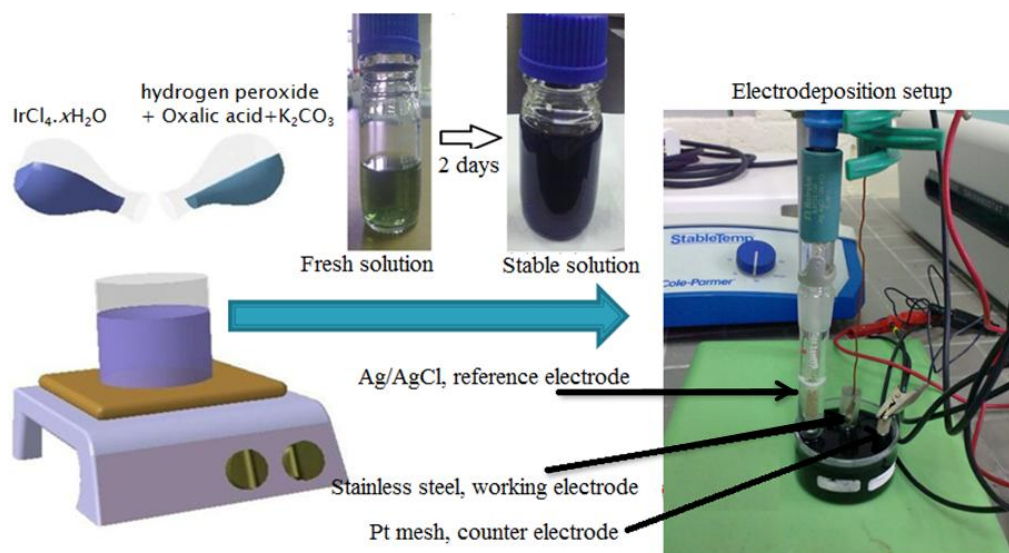


Figure 2. Solution preparation and electrodeposition setup

As shown in figure 3, a three electrode cell was used in this study. An iridium oxide layers were deposited on stainless steel working electrode by using an Ag/AgCl reference electrode and a mesh Pt counter electrode. A cyclic voltammetry method between -0.5 to 0.65 V (vs. Ag/AgCl) was applied at different cycles and sweep rates as shown in Table 1.

A potentiostat/galvanostat (Autolab, Metrohm, model PGSTAT 128N) was used in cyclic voltammetry deposition (CV) of EIROF and in CV, electrochemical impedance spectroscopy (EIS), open circuit potential (OCP) measurements. A conventional glass pH electrode was used for pH sensor calibration. In this study, all impedance spectra were measured with a 10-mV (Amplitude, rms) AC

sinusoidal signal in the frequency range of 0.01 Hz to 10 kHz. NOVA-1.8 software was used to do the EIS measurements and curve fitting analysis.

The potential response of EIROF in standard pH solution buffer (4, 7, and 9) was measured by potentiostat at room temperature.

The electrodeposited iridium oxide was characterized by CV, Atomic Force Microscopy (AFM), Field Emission Scanning Electron Microscopy (FESEM) (HITACHI), and Energy-Dispersive X-ray spectroscopy (EDX).

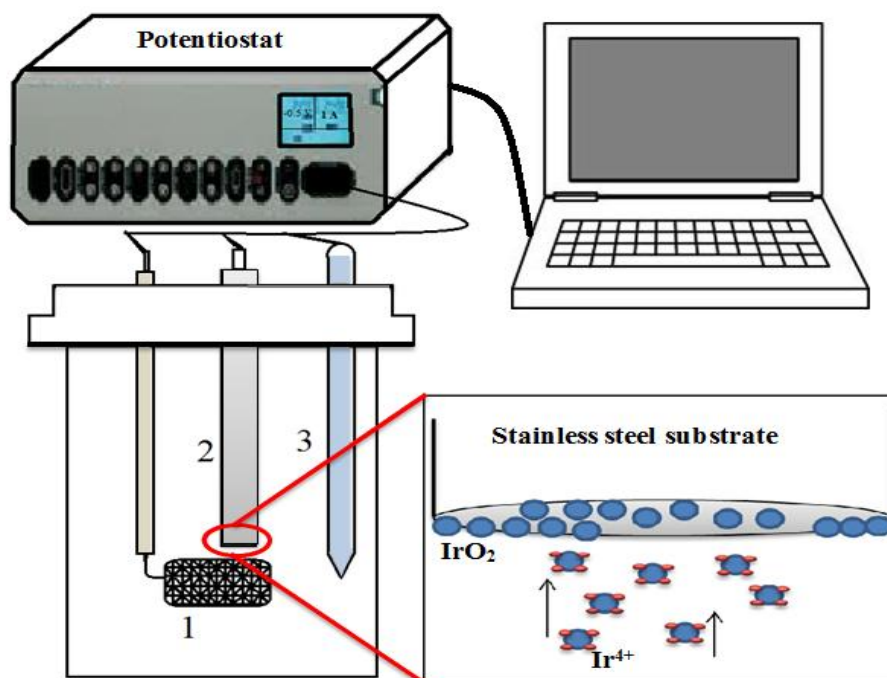


Figure 3. Schematic diagram of an electrodeposition setup: (1) Pt mesh counter electrode, (2) stainless steel (working electrode), (3) Ag/AgCl reference electrode

3. RESULTS AND DISCUSSION

According to Table 1, two scan rates (50 and 200 mV/s) and two cycles (100 and 500 cycles) were used in cyclic voltammetry method to deposit iridium oxide layer on stainless steel substrate. Growing of iridium oxide layer on stainless steel with increasing cycle from 1 to 500 cycles is demonstrated in figure 4 which shows that IrO₂ layer thickness increased by increasing cyclic number. The result is summarized in Table 1. All electrodeposited surfaces were blue colour and free of crack.

The thickness of IrO₂ layer was measured by using atomic force microscopy. As shown in Table 1, cathodic charge storage capacity (CSC_C) as a representative of IrO₂ thickness is a function of cycle number and scan rate. IrO₂ thickness increased with increasing cycle number and decreasing scan rate.

Table 1. Experimental design for IrO₂ electrodeposition on stainless steel

Sample code	Scan Rate (mV/s)	T(°C)	Cycle	CSC _C (mC/cm ²)	Sensitivity (mV/pH)
a	50	25	100	2.739 x 10 ⁻⁴	-73.84
b	200	25	100	1.162 x 10 ⁻⁴	-73.31
c	200	25	500	2.051 x 10 ⁻⁴	-74.5
d	50	25	500	10.385 x 10 ⁻⁴	-69.98

According to figure 4, it is worthy to mention that with increasing cycles in cyclic voltammetry method of IrO₂ electrodeposition, CSC_C of electrodes will increase which is a critical characteristic in some application of IrO₂ electrodes such as neural recording and stimulation. The CSC_C of the EIROF can be calculated using the time integral of the cathodic current during a potential sweep between 0.80 and -0.60V (vs. Ag/AgCl) at a scan rate of 50 mV/s (figure 5). According to literature CSC_C is directly proportional with IrO₂ thickness [21].

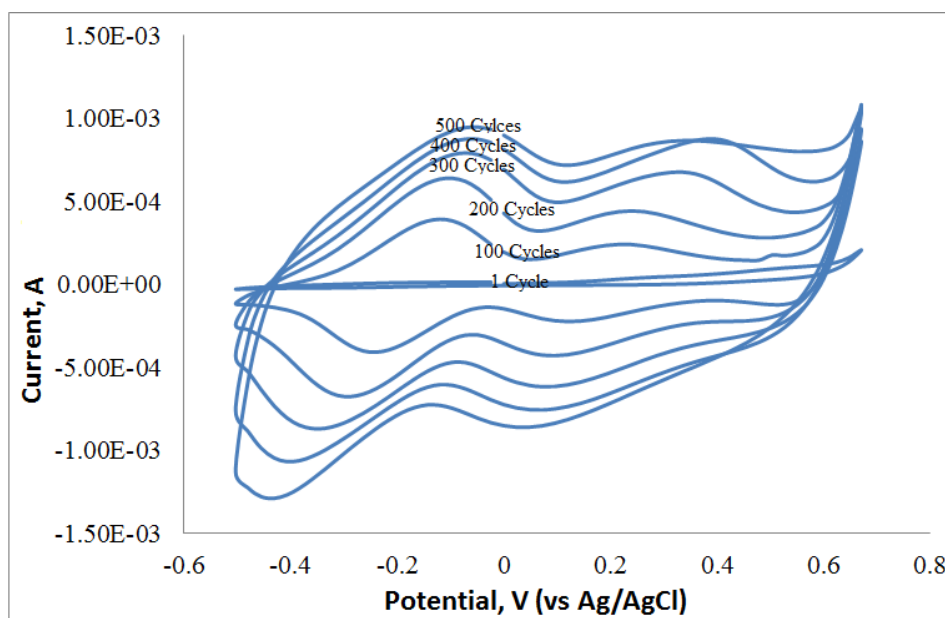


Figure 4. Growth of iridium oxide on stainless steel substrate by cyclic voltammetry method at a scan rate of 50 mV/s.

The open circuit potential (OCP) of all fabricated pH sensors were measured versus three standard pH (4, 7, and 9) buffer solution. As figure 6 shows all sensors presented a good linear relation (R²=0.99) and super-Nernstian response value in range of -69.9 to -74.5 mV/pH unit. Different oxidation state is the main reason for the sensitivity deviations between sensors [23]. It can be concluded that pH response increased whether decreasing electrodeposition cycles or increasing scan rate. Sensor *b* had a faster response time due to its thinner IrO₂ layer, although it was not very stable in

pH 2 buffer solution. The sensitivity of the pH electrodes stayed almost constant during 6–7 weeks storage time in pH 7 buffer solution.

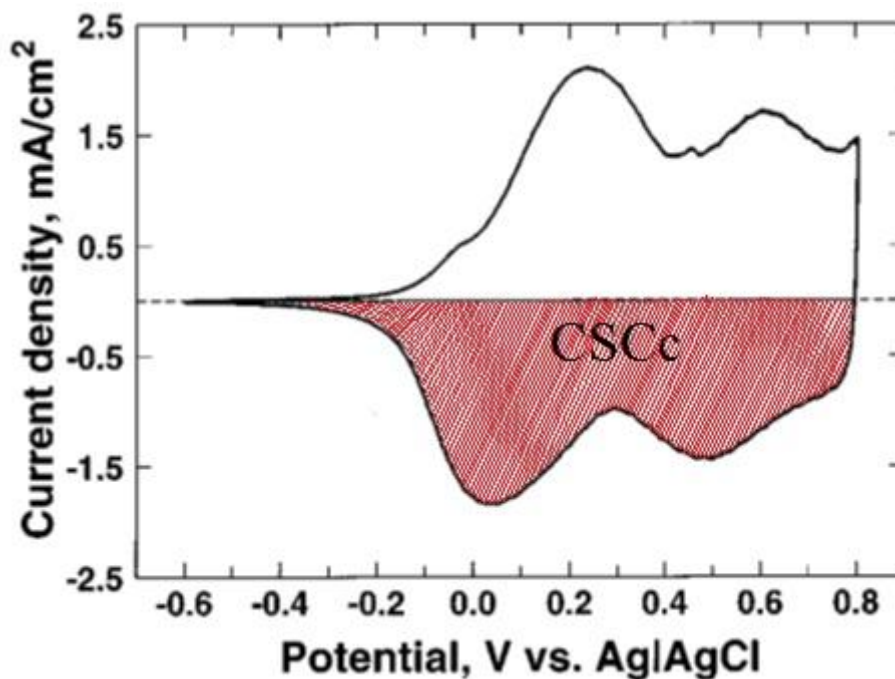


Figure 5. Area used to calculate CSC_C in EIROF electrode

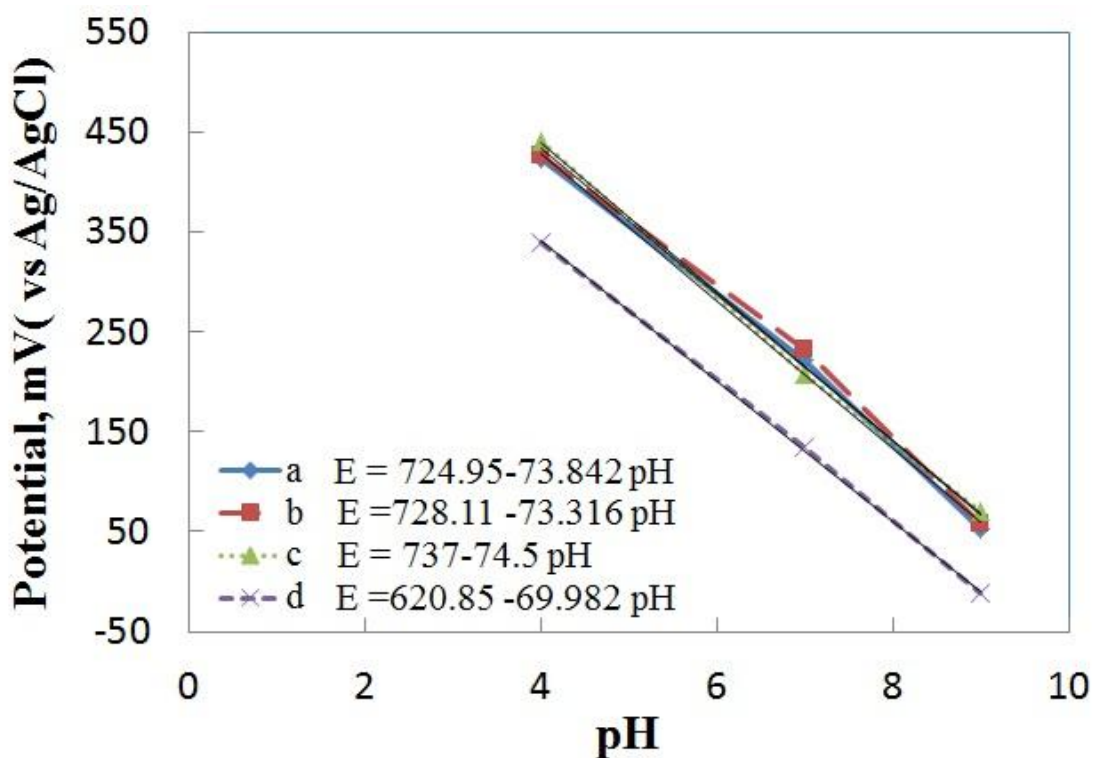


Figure 6. Typical potentiometric response of the EIROF electrode to a series of universal buffer solutions

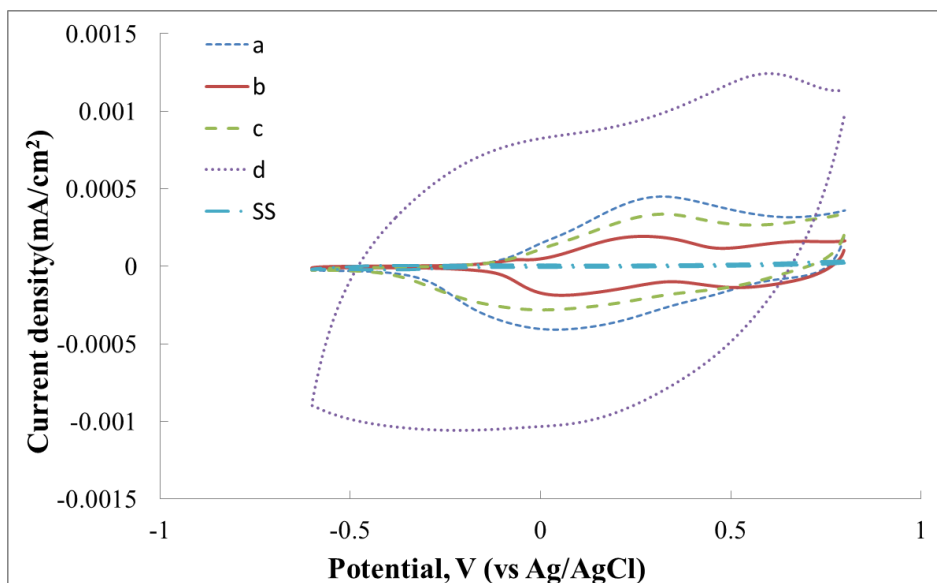


Figure 7. Cyclic voltammetry of bare stainless steel and EIROF electrodes in pH 7 standard buffer solution at a scan rate of 50 mV/s.

Cyclic voltammograms of bare stainless steel and EIROF electrodes were given in Figure 7. The redox reactions peak of iridium oxides is indicated in CV of EIROF, which is included in the transfer of ions through the electrode/electrolyte interface. The CSC_C of the IrO_2 coated stainless steel electrodes is very larger than bare stainless steel electrode. The CV result showed scan rate and number of cycles of CV electrodeposition method have a significant effect on cyclic voltammetry characteristics of EIROF.

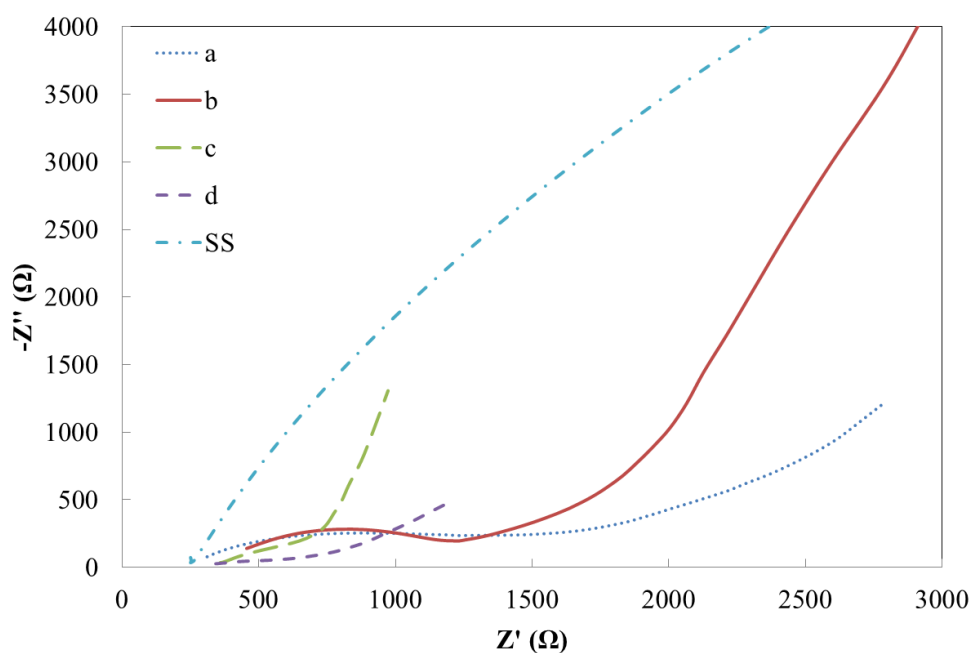


Figure 8. Nyquist plot of EIROF electrode on stainless steel

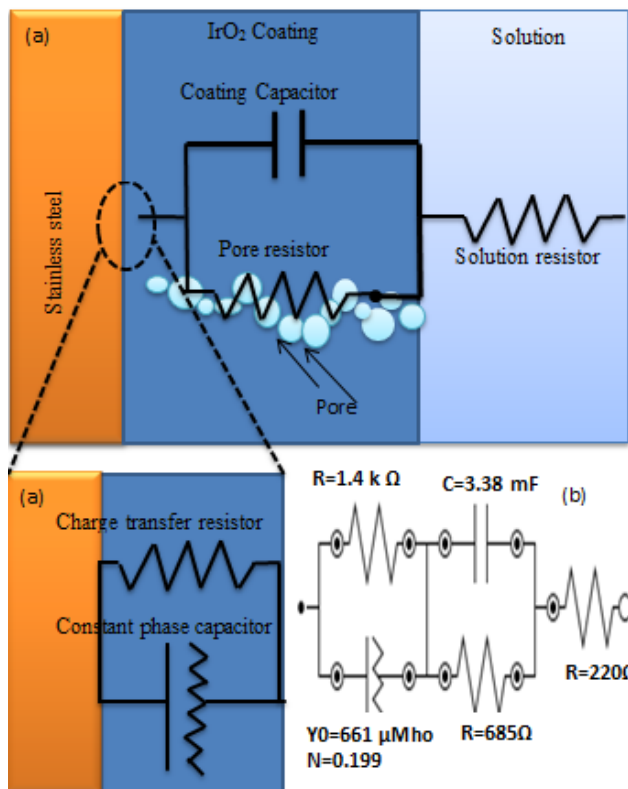


Figure 9. Equivalent circuit models; (a) circuit model of IrO₂ coated stainless steel physical properties, (b) representing an equivalent circuit model of fitting EIS data

The electrochemical impedances of bare stainless steel and EIROF electrodes in pH 7 standard buffer solution are illustrated in Figure 8 and 10. The impedance data are presented as Nyquist plot (figure 8) and Bode plots of \log_{10} Impedance modulus $[Z (\Omega)]$ versus \log_{10} Frequency (Hz) (figure 10). Equivalent circuit model of fitting EIS data of figure 8 is illustrated in figure 9. The low coating resistor of IrO₂ coating is because of its high conductivity. The benefit of iridium oxide in lowering electrode impedance is shown in these figures.

A constant phase element (CPE) was selected in equivalent circuit model which shows a dispersive double layer capacitance. CPE is a substitute for normal capacitor when electrode surface is non-homogenous. The CPE impedance is represented as the following equation [16, 24]:

$$Z_{CPE} = \frac{1}{Q(i\omega)^\alpha} \tag{2}$$

Where Q is a constant, i is the imaginary number, ω is the angular frequency and α is a parameter that has a value between 0 and 1. EIS result shows that increasing cycles has more effect on lowering impedance than increasing scan rate. Electrodes which were coated by electrodeposition at different scan rate demonstrated similar behavior in impedance recording. It is worthy mention that at frequencies below 10⁴ Hz, the impedance decreases with increasing film thickness.

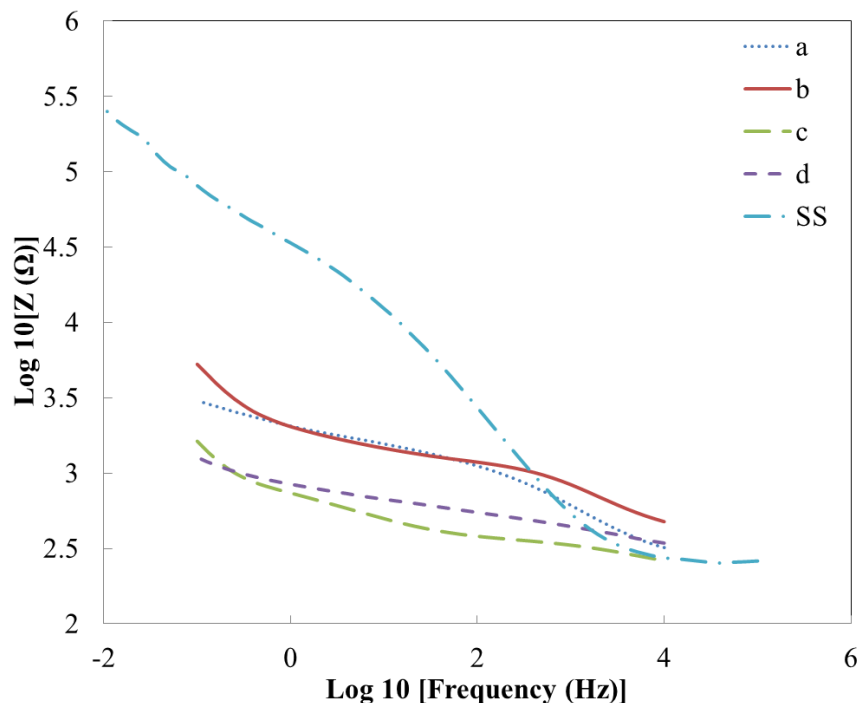


Figure 10. AC Impedance of bare stainless steel and EIROF electrodes as a function of cycles and scan rate

Figure 11 shows EDX analysis of EIROF electrodes. A table indicating element value is demonstrated in this figure which shows iridium and oxygen has more weight percent in EIROF component.

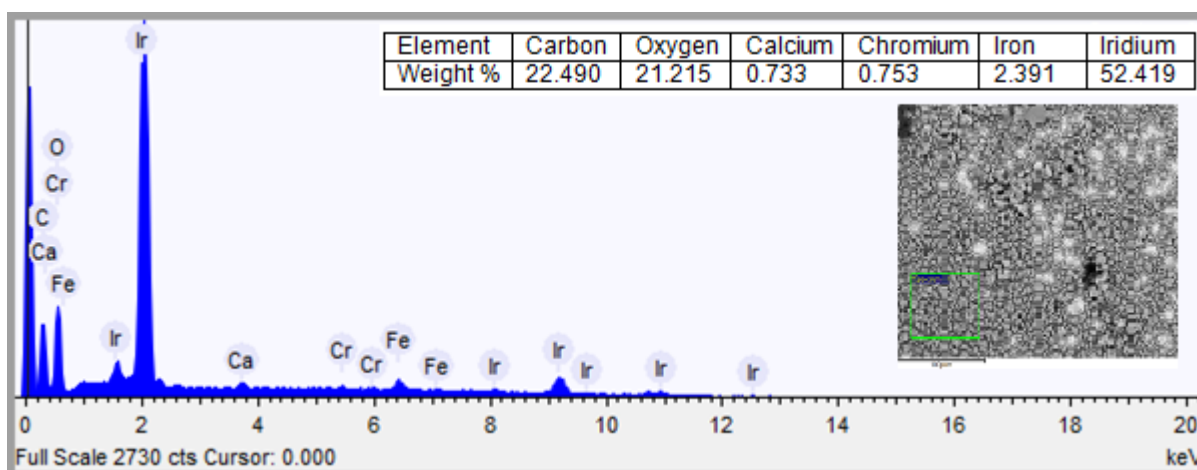


Figure 11. EDX spectra of iridium oxide electrodeposited on stainless steel substrate

FESEM images of EIROF surface is shown in figure 12. The cracks that are indicated in FESEM images result from layer dehydration in the SEM vacuum chamber [25]. A cauliflower

appearance was achieved in thicker films. More roughness of EIROF leads to higher surface area which results in more surface exposure to test environment and better response to pH changes.

A morphology feature of IrO₂ layer is shown in figure 13. 3D image of pH sensitive IrO₂ layer shows that it was a unique and free of crack coating.

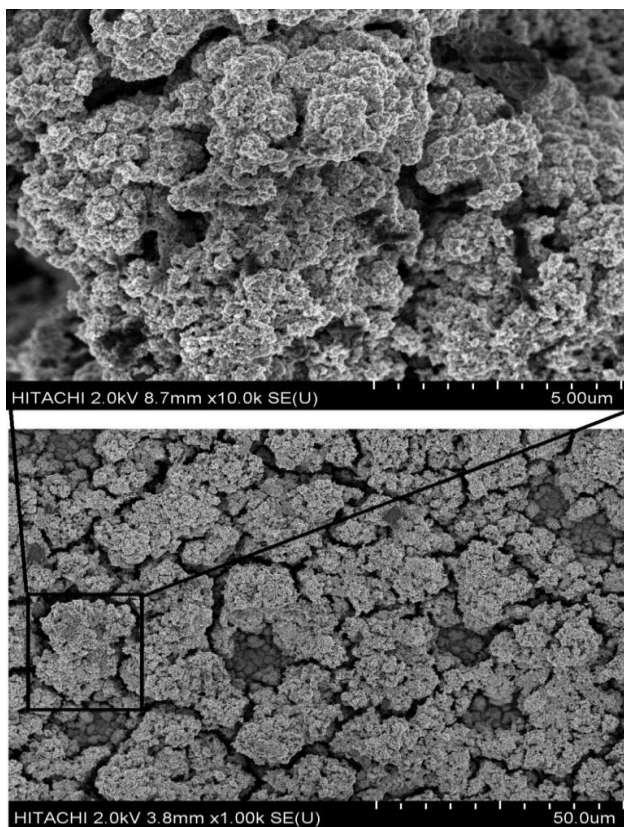


Figure 12. FESEM images of EIROF electrode

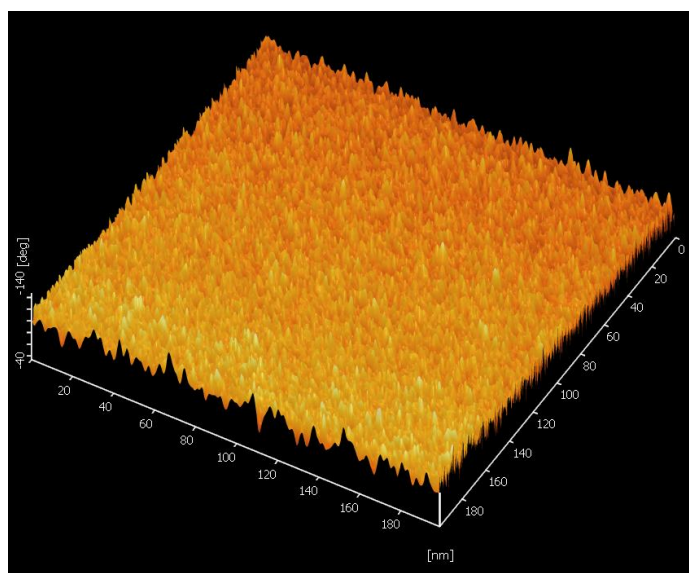


Figure 13. AFM image of iridium oxide fabricated by CV.

4. CONCLUSION

Iridium oxide was electrodeposited on a stainless steel substrate by cyclic voltammetry method. The effect of cycle number and scan rates on iridium oxide characterization was investigated. A blue and homogenous surface was observed after electrodeposition for all cases.

All fabricated pH sensor had a super-Nernstian response value in range of -69.9 to -74.5 mV/pH unit. Thinner pH sensors showed faster pH response.

Electrochemical results indicated iridium oxide decreased electrode impedance which was in direct relation with its thickness. Cycle numbers has more effect on EIROF electrode characteristics than scan rate. Low resistance of IrO₂ in the equivalent circuit models is an evidence for high electrical conductivity of EIROF.

ACKNOWLEDGMENTS

We would like to acknowledge Universiti Teknologi PETRONAS and Ministry of Higher Education (ERGS Grant No: 158200327) for their financial support.

References

1. H. Yang, S. K. Kang, D. H. Shin, H. Kim, and Y. T. Kim. 2003. IEEE.
2. R. K. Franklin, S. Joo, S. Negi, F. Solzbacher, and R. B. Brown. *IEEE SENSORS 2009 Conference*. 2009. IEEE.
3. R. A. Macur, Milwauki, Wis., US Patent 3,726,777 (1973)
4. D. O'Hare, K. H. Parker, and C. P. Winloves, *Medical engineering & physics* 28(2006) 982
5. J. C. Chiao and W. D. Huang, US2011/0140703 (2010)
6. P. Huang and K. G. Kreider, 1988, Nuclear Regulatory Commission, Washington, DC (USA). Div. of Engineering; National Bureau of Standards, Washington, DC (USA). Center for Chemical Engineering.
7. K. Kreiders, *Sensors and Actuators B: Chemical* 5(1991) 165
8. R. Prasads, NACE Int. Conference, (2000) 00390
9. Z. Lewandowski, T. Funk, F. Roe, B. J. Little, J. Kearns, and B. Littles, *ASTM International* 1232(1994) 61
10. B. J. Little, Z. Lewandowski, T. Funk, and F. Roe, *Spatial Distribution of pH at Mild Steel Surfaces Using an Iridium Oxide Microelectrode*, 1994, DTIC Document.
11. Y. J. Kim, Y. C. Lee, B. K. Sohn, J. H. Lee, and C. S. Kims, *J. Korean Phys. Soc.* 43(2003) 769
12. H. Quan, W. Kim, K. Chung, and J. Parks, *Bull. Korean Chem. Soc.* 26(2005) 1565.
13. I. Song, K. Fink, and J. Payers, *Corrosion, NACE Inter.* 54(1998) 98010013.
14. T. Arikawa, Y. Takasu, Y. Murakami, K. Asakura, and Y. Iwasawas, *The Journal of Physical Chemistry B* 102(1998) 3736
15. K. Yamanakas, *Japanese journal of applied physics* 28(1989) 632-637.
16. Y. Lu, T. Wang, Z. Cai, Y. Cao, H. Yang, and Y. Y. Duans, *Sensors and Actuators B: Chemical* 137(2009) 334
17. M. Pikulski and W. Gorskis, *Analytical chemistry* 72(2000) 2696
18. C. Terashima, T. N. Rao, B. V. Sarada, N. Spataru, and A. Fujishimas, *Journal of Electroanalytical Chemistry* 544(2003) 65
19. I. A. Ges, B. L. Ivanov, D. K. Schaffer, E. A. Lima, A. A. Werdich, and F. J. Baudenbachers, *Biosensors and Bioelectronics* 21(2005) 248

20. S. A. M. Marzouks, *Analytical chemistry* 75(2003) 1258
21. R. D. Meyer, S. F. Cogan, T. H. Nguyen, and R. D. Rauhs, *Neural Systems and Rehabilitation Engineering*, IEEE Transactions on 9(2001) 2
22. C. C. Mayorga Martinez, R. E. Madrid, and C. J. Felices, *Sensors and Actuators B: Chemical* 133(2008) 682
23. W. D. Huang, L. C. Hsu, J. Wang, T. Ativanichayaphong, S. Deb, M. Chiao, and J. Chiao. *Smart Materials, Nano-and Micro-Smart Systems*. 2008. International Society for Optics and Photonics.
24. S. S. Thanawala, R. J. Baird, D. G. Georgiev, and G. W. Auners, *Applied Surface Science* 254(2008) 5164
25. J. D. Blakemore, N. D. Schley, M. N. Kushner-Lenhoff, A. M. Winter, F. D'Souza, R. H. Crabtree, and G. W. Brudvigs, *Inorganic Chemistry* 51(2012) 7749